

First Results from the Large Area Lyman Alpha Survey

James E. Rhoads¹, Sangeeta Malhotra^{2,3}, & Arjun Dey²

Kitt Peak National Observatory

Daniel Stern⁴ & Hyron Spinrad

Astronomy Department, University of California, Berkeley, CA 94720

Buell T. Jannuzi

National Optical Astronomy Observatories

ABSTRACT

We report on a new survey for $z \approx 4.5$ Lyman- α sources, the Large Area Lyman Alpha (LALA) survey. Our survey achieves an unprecedented combination of volume and sensitivity by using narrow-band filters on the new 8192^2 pixel CCD Mosaic Camera at the 4 meter Mayall telescope of Kitt Peak National Observatory.

Well-detected sources with flux and equivalent width matching known high redshift Lyman- α galaxies (i.e., observed equivalent width $EW > 80\text{\AA}$, $2.6 < (\text{line} + \text{continuum flux}) / (10^{-17} \text{ erg cm}^{-2} \text{ s}^{-1}) < 5.2$, and $\delta(EW)/EW < 0.25$) have an observed surface density corresponding to 11000 ± 700 per square degree per unit redshift at $z = 4.5$. Spatial variation in this surface density is apparent on comparison between counts in $6561 \pm 40\text{\AA}$ and $6730 \pm 40\text{\AA}$ filters.

Early spectroscopic followup results from the Keck telescope included three sources meeting our criteria for good Lyman- α candidates. Of these, one is confirmed as a $z = 4.52$ source, while another remains consistent with either $z = 4.55$ or $z = 0.81$. We infer that 30 to 50% of our good candidates are *bona fide* Lyman- α emitters, implying a net density of ~ 4000 Lyman- α emitters per square degree per unit redshift.

Subject headings: galaxies

¹present address: Space Telescope Science Institute, 3700 San Martin Drive, Baltimore, MD 21218 ; rhoads@stsci.edu

²Hubble Fellow

³present address: Johns Hopkins University

⁴present address: Jet Propulsion Laboratory, California Institute of Technology, Mail Stop 169-327, Pasadena, CA 91109

1. Introduction

More than three decades ago Partridge and Peebles (1967) predicted that galaxies in their first throes of star-formation should be strong emitters in the Lyman- α line. Their predictions were optimistic, based on converting roughly 2% of gas into stars in 3×10^7 years in Milky Way sized galaxies, which translates into a luminosity of 6×10^{44} ergs $^{-1}$. These objects are also expected to be common - if all the L^* galaxies have undergone a phase of rapid star-formation one should see a surface density of about $3 \times 10^3 \times (\Delta t / (3 \times 10^7 \text{ yr})) \text{ deg}^{-2}$ (Pritchett 1994). Searches based on these expectations did not detect Lyman- α emitters (LAEs). (See review by Pritchett 1994; Koo & Kron 1980; Pritchett & Hartwick 1987, 1990; Cowie 1988; Rhea et al 1989; Smith et al 1989; Lowenthal et al 1990; Wolfe et al 1992; De Propriis et al 1993; Macchetto et al 1993; Møller & Warren 1993; Djorgovski & Thompson 1992; Djorgovski, Thompson, & Smith 1993; Thompson, Djorgovski, & Trauger 1992; Thompson et al 1993; Thompson, Djorgovski, & Beckwith 1994; Thommes et al 1998.)

Only recently have Lyman- α emitters been observed, albeit at luminosity levels roughly a hundred times lower than the original prediction. These Lyman- α emitters have been found from both deep narrow band imaging surveys (Cowie & Hu 1998; Hu, Cowie & McMahon 1998; Hu, McMahon, & Cowie 1999; Kudritzki et al 2000), and from deep spectroscopic surveys (Dey et al 1998; Manning et al 2000; but see Stern et al 2000). Weak Lyman- α emitters have also been found through targeted spectroscopy of Lyman break objects (e.g., Steidel et al 1996, Lowenthal et al 1997). The lower luminosity in the Lyman- α line may be because of attenuation by dust if chemical enrichment is prompt; or because the star-forming phase is more protracted; or because the star-formation happens in smaller units which later merge. The first two scenarios will give a smaller equivalent width than early predictions, while the last scenario results in low luminosities but high equivalent width.

Dust effects are expected to be severe— even a small amount of dust can greatly attenuate this line, because it is resonantly scattered. However, two factors can help the Lyman- α photons escape. If Lyman- α photons are produced in diffuse regions of a clumpy interstellar medium, they can simply scatter off the dense clumps and escape (Neufeld 1991), and some geometries can even lead to an increase in the equivalent width of the line. Secondly, energetic winds are seen in low- z Lyman- α emitters (Kunth et al 1998). These can displace the neutral gas and doppler-shift the peak wavelength of the resonant scattering, thereby reducing the amount of scattering and the path length for interaction with dust.

Detailed predictions for luminosities and surface densities of LAEs using a Press-Schechter formalism and exploring a range of dust obscuration and star-formation time scales have been explored by Haiman and Spaans (1999), who are able to reproduce the surface densities of LAEs reported by Hu et al (1998) with a wide range of models. In order to narrow down the range of possibilities and characterize the high redshift Lyman- α population, better statistics over a wide range of flux and source density are needed.

2. Narrow Band Imaging Survey

An efficient search for Lyman- α emitters (and other emission line galaxies) was started in 1998 using the CCD Mosaic Camera at the Kitt Peak National Observatory’s 4m Mayall telescope. The Mosaic camera has eight 2048×4096 chips in a 4×2 array comprising a $36' \times 36'$ field of view. The final area covered by the LALA survey is 0.72 square-degrees in two MOSAIC fields centered at 14:25:57 +35:32 (2000.0) and 02:05:20 -04:55 (2000.0). Five overlapping narrow band filters of width $\text{FWHM} \approx 80\text{\AA}$ are used. The central wavelengths are 6559, 6611, 6650, 6692, and 6730 \AA , giving a total redshift coverage $4.37 < z < 4.57$. This translates into surveyed comoving volume of 8.5×10^5 comoving Mpc^3 per field for $H_0 = 70 \text{ km s}^{-1} \text{ Mpc}^{-1}$, $\Omega = 0.2$, $\Lambda = 0$. About 70% of the imaging at $z \approx 4.5$ is complete, and an extension of the survey to $z > 5$ is planned. In about 6 hours per filter per field we are able to achieve line detections of about $2 \times 10^{-17} \text{ erg cm}^{-2} \text{ s}^{-1}$. The survey sensitivity varies with seeing. Broadband images of these fields in a custom B_w filter ($\lambda_0 = 4135\text{\AA}$, $\text{FWHM} = 1278\text{\AA}$) and the Johnson-Cousins R , I , and K bands are being taken as part of the NOAO Deep Widefield Survey (Jannuzi & Dey 1999).

The images were reduced using the MSCRED package (Valdes & Tody 1998; Valdes 1998) in the IRAF environment (Tody 1986, 1993), together with assorted custom IRAF scripts. In addition to standard CCD data reduction steps (overscan subtraction, bias frame subtraction, and flatfielding), it was necessary to remove crosstalk between pairs of CCDs sharing readout electronics and to remove a ghost image of the telescope pupil. Astrometry of USNO-A catalog stars was used to interpolate all chips and exposures onto a single coordinate grid prior to combining final images. Cosmic ray rejection is of particular importance in a narrowband search for emission line objects. We therefore identified cosmic rays in individual images using a digital filtering method (Rhoads 2000) and additionally applied a sigma clipping algorithm at the image stacking stage. Weights for each exposure were determined using the method of Fischer & Kochanski (1994), which accounts for sky level, transparency, and seeing to optimize the signal to noise level for compact sources in the final image.

Catalogs were generated using the SExtractor package (Bertin & Arnouts 1996). Fluxes were measured in $2.32''$ (9 pixel) diameter apertures, and colors were obtained using matched $2.32''$ apertures in registered images that had been convolved to yield matched point spread functions.

3. Spectroscopic Observations

Spectroscopic followup of a cross-section of emission line candidates was obtained with the LRIS instrument (Oke et al 1995) at the Keck 10m telescope on 1999 June 13 (UT). Two dithered exposures of 1800 seconds each were obtained through a single multislit mask in good weather.

These data were reduced using a combination of standard IRAF ONEDSPEC and TWODSPEC tasks together with the homegrown slitmask reduction IRAF task “BOGUS” (Stern,

Bunker, & Stanford, private communication) for reducing LRIS data.

4. The emission line source population

Our imaging data yield numbers of sources as a function of their fluxes in several filters, from which we can construct number densities as a function of magnitudes, colors, and equivalent widths. In order to gracefully handle sources that are not detected in all filters, we have chosen to use “asinh magnitudes” (Lupton, Gunn, & Szalay 1999), which are a logarithmic function of flux for well detected sources but approach a linear function of flux for weak or undetected sources. Figure 1 shows the color-magnitude diagram for the 6559Å ($\pm 40\text{\AA}$) and R filters. The color scatter achieved for bright sources ($R < 22$) is 0.10 magnitudes (semi-interquartile range). This includes the true scatter in object colors, and is therefore a firm upper limit on the scatter introduced by any residual systematic error sources, which we expect to be a few percent at worst.

To sharpen our focus on the high redshift Lyman- α population, we identify the range of parameter space occupied by known $z > 3$ Lyman- α emitters. These sources have typical observed equivalent widths $\gtrsim 80\text{\AA}$ and line+continuum fluxes $\lesssim 5 \times 10^{-17} \text{ erg cm}^{-2} \text{ s}^{-1}$ (adjusted to $z = 4.5$ and measured in an 80Å filter).

We further want to restrict attention to sources with sufficiently reliable detections that the number of false emission line candidates is a small fraction of the total candidate sample. The data set includes many continuum sources ($\sim 1.4 \times 10^4$ in the flux range above). It is expected to contain a few hundred emission line sources, based on earlier source counts from smaller samples (Hu et al 1998) and on our own findings (below). The fraction of continuum sources with measured equivalent widths above some threshold EW_0 can be calculated as a function of signal to noise level n and filter width $\Delta\lambda$: The measured equivalent width for a source with no line emission or absorption in the narrowband filter will be $0 \pm \Delta\lambda/n$. Thus, a false positive becomes an $m\sigma$ event, where $m = n \times EW_0/\Delta\lambda$. Our sample would be reasonably safe from contamination with $m = 3$, which would correspond to about 20 false positives in a sample of 14000 sources; and very safe for $m \gtrsim 4$, corresponding to < 1 false positive in 14000 sources. We have conservatively chosen detection thresholds $n = 5$ and $EW_0 = \Delta\lambda = 80\text{\AA}$, which gives $m = 5$. This keeps the number of false positives small even when the foregoing analysis is expanded to include errors in the continuum flux (which increase photometric error in the color by a factor $\sim \sqrt{2}$) and a realistic distribution of equivalent widths for the low- z galaxy populations. As a further check on our sample, we use the photometric color error estimates from SExtractor to demand that the source be an emission line source at the 4σ level.

Combining all of these requirements, the final criteria for good candidates in our survey become $EW > 80\text{\AA}$, $\delta(EW)/EW \leq 0.25$, and $2.6 < f_{17} < 5.2$, where $f_{17} \equiv f/(10^{-17} \text{ erg cm}^{-2} \text{ s}^{-1})$. There are 225 such sources detected in the 6559Å filter in a solid angle of 0.31 square degree and redshift range $\delta z = 0.07$. This corresponds to 11000 good candidate Lyman- α emitters per square

degree per unit redshift. The precise upper flux cutoff used is somewhat arbitrary, but including sources with larger fluxes in our list of good candidates has little effect on the total source counts.

The final 6730Å image had a broader PSF than the 6559Å image, and consequently a reduced effective sensitivity. In addition, it samples a slightly higher redshift, resulting in an 0.08 magnitude increase in distance modulus ($q_0 = 0.1$, $\Lambda = 0$). Accounting for both effects, the matched flux range is $3.45 < f_{17} < 5.2$ at 6559Å and $3.2 < f_{17} < 4.8$ at 6730Å. The corresponding counts are 70 candidates at 6730Å, and 104 candidates at 6559Å. Thus, the source density in directly comparable luminosity bins varies by a factor of 1.5, a difference that is significant at about the 3σ level. We interpret this as a likely signature of large scale structure in the Lyman- α emitter distribution at $z \approx 4.5$. The comoving distance between the centers of the two redshift slices is 72Mpc, while the thickness of each slice is 36Mpc and the transverse comoving size 89Mpc (again assuming $H_0 = 70 \text{ km s}^{-1} \text{ Mpc}^{-1}$, $\Omega = 0.2$, $\Lambda = 0$). Comparable variations have been observed in the density of Lyman break galaxies at $z \approx 3.1$ (Steidel et al 1998).

5. Spectroscopic results

Our spectroscopic followup sampled a wide range of flux and equivalent width in order to characterize the different populations of sources with extreme narrowband colors, and to thereby tune candidate selection criteria for future spectroscopic observations. Those sources with 5σ narrowband detections and photometrically measured $\text{EW} > 65\text{\AA}$ were all confirmed as emission line objects at the narrowband wavelength. In total, we detected two [O III] $\lambda 5007$ emitters at $z = 0.34$, three [O II] $\lambda 3727$ emitters at $z = 0.77$ and $z = 0.81$, one confirmed Lyman- α (1215Å) emitter at $z = 4.516$, and one source that could either be Lyman- α at $z = 4.55$ or [O II] $\lambda 3727$ at $z = 0.81$. We also found a $z = 2.57$ galaxy with emission lines of C IV $\lambda 1549$, He II $\lambda 1640$, and O III $\lambda 1663$. This source may have been included in the narrowband candidate list (with $\text{EW} = 36\text{\AA}$) because of a weak spectral break around 6560Å. Finally, we found a few serendipitous emission line sources in the slit spectra. One of these is a single-line source with large equivalent width, possibly Lyman- α at $z = 3.99$. Spectra of two interesting sources are shown in figure 2.

6. Discussion: The Lyman- α source population

By combining our imaging survey with these spectroscopic results, we can estimate the source density of Lyman- α emitters passing our selection cut. Our spectra included three sources fulfilling the criteria given above for good candidates. Of these, one was confirmed as a $z = 4.52$ Lyman- α source. A second remains a candidate $z = 4.55$ source, but is more conservatively interpreted as a $z = 0.81$ [O II] emitter on the basis of a rather strong continuum on the blue side of the line. The third is a clear $z = 0.34$ [O III] emitter. We therefore estimate that roughly 1/3 to 1/2 of the good candidates will be confirmed as Lyman- α sources, yielding ~ 4000 emitters per square degree per

unit redshift. This is compatible with earlier measurements from smaller volumes (Hu et al 1998) after accounting for differences in flux threshold.

Our measurement is distinct from previous efforts in the field for its basis in a large number of candidate emitters. Poisson errors in our source counts are of order $\pm 7\%$. This is smaller than the variations observed in the comparison of two filters (of order $\pm 40\%$). By combining observations in multiple fields, we will be able to average over local fluctuations in number densities effectively. When completed, the LALA survey will yield comoving volume of $\sim 2 \times 10^6 \text{Mpc}^3$ (§2) and a sample of several hundred LAEs, and will allow the luminosity function, equivalent width distribution, and correlation function of this population to be determined for the first time.

We thank Andy Bunker and Steve Dawson for help with the spectroscopic observations and Frank Valdes for writing and helping with the MSCRED package in IRAF. JER's research is supported by a Kitt Peak Postdoctoral Fellowship and by an STScI Institute Fellowship. SM's research is supported by NASA through Hubble Fellowship grant # HF-01111.01-98A from the Space Telescope Science Institute, which is operated by the Association of Universities for Research in Astronomy, Inc., under NASA contract NAS5-26555.

REFERENCES

- Bertin, E. and Arnouts, S., 1996, A&AS 117,393
- Cowie, L. L. 1988, in "The Post-Recombination Universe", Ed. N. Kaiser & A. N. Lasenby (Dordrecht, Kluwer) p. 1
- Cowie, L. L., & Hu, E. M. 1998, AJ 115, 1319
- De Propris, R. Pritchett, C. J., Hartwick, F. D. A., & Hickson, P. 1993, AJ 105, 1243
- Dey, A., Spinrad, H., Stern, D., Graham, J. R., & Chaffee, F. H. 1998, ApJ 498, 93
- Djorgovski, S., & Thompson, D. J. 1992, in "The Stellar Populations of Galaxies," IAU Symposium 149, ed. B. Barbuy & A. Renzini (Dordrecht, Kluwer), p. 337
- Djorgovski, S., Thompson, D. J., & Smith, J. D. 1993, in "First Light in the Universe," ed. B. Rocca-Volmerange, M. Dennefeld, B. Guiderdoni, & J. Tran Thanh Van (Gif sur Yvette, Editions Frontières), p. 67
- Fischer, P., & Kochanski, G. P. 1994, AJ 107, 802
- Hu, E. M., Cowie, L. L., & McMahon, R. G. 1998, ApJ 502, L99
- Jannuzi, B. T., & Dey, A., 1999, in "Photometric Redshifts and High Redshift Galaxies", ASP Conference Series, Vol. 191, editors R. J. Weymann, L. J. Storrie-Lombardi, M. Sawicki, and R. J. Brunner, p.111
- Koo, D. C., & Kron, R. G. 1980, PASP 92, 537

- Kudritzki, R.-P., et al 2000, in preparation
- Landolt, A. U. 1992, AJ 104, 340
- Lowenthal, J. D., Hogan, C. J., Leach, R. W., Schmidt, G. D., & Foltz, C. B. 1990, ApJ 357, 3
- Lowenthal, J. D., Koo, D. C., Guzman, R., Gallego, J., Phillips, A. C., Faber, S. M., Vogt, N. P., Illingworth, G. D., & Gronwall, C. 1997, ApJ 481, 673
- Lupton, R. H., Gunn, J. E., & Szalay, A. S. 1999, aj 118, 406.
- Manning, xx, et al 2000, astro-ph/0002239
- Kunth, D., Mas-Hesse, J. M., Terlevich, E., Terlevich, R., Lequeux, J., & Fall, S. M. 1998, A&A 334, 11
- Macchetto, F., Lipari, S., Giavalisco, M., Turnshek, D. A., & Sparks, W. B. 1993, ApJ 404, 511
- Møller, P., & Warren, S. J. 1993, A&A 270, 43
- Oke, J.B. et al 1995, PASP, 107, 375
- Pritchett, C. J. 1994, PASP 106, 1052
- Pritchett, C. J., & Hartwick, F. D. A. 1987, ApJ 320, 464
- Pritchett, C. J., & Hartwick, F. D. A. 1990, ApJ 355, L11
- Rhee, G. F. R. N., Webb, J. K., & Katgert, P. 1989, A&A 217, 1
- Rhoads, J. E. 2000, PASP in press (May 2000 issue)
- Smith, H. E., Cohen, R. D., Burns, J. E., Moore, D. J., & Uchida, B. A. 1989, ApJ 347, 87
- Steidel, C.C., Giavalisco, M., Pettini, M., Dickinson, M., & Anderson, K. L. 1996, ApJ 462, L17
- Steidel, C. C., Adelberger, K. L., Dickinson, M., Giavalisco, M., Pettini, M., & Kellogg, M. 1998, ApJ 492, 428.
- Stern, D., & Spinrad, H. 1999, PASP 111, 1475
- Stern, D., et al 2000, astro-ph/0002241
- Thompson, D., Djorgovski, S., & Trauger, J. 1992, in “Cosmology and Large-Scale Structure in the Universe,” ASP Conference Series, Vol. 24 (San Francisco, ASP), p. 147
- Thompson, D., Djorgovski, S., Trauger, J., & Beckwith, S. 1993, in “Sky Surveys: Protostars to Protogalaxies,” ASP Conference Series, Vol. 43, ed. B. T. Soifer (San Francisco, ASP), P. 185
- Thommes, E., Meisenheimer, K., Fockenbrock, R., Hippelein, H., Röser, H.-J., & Beckwith, S. 1998, MNRAS 293, L6
- Thompson, D., Djorgovski, S., & Beckwith, S. 1994, AJ 107, 1
- Tody, D. 1986, Proc. SPIE Instrumentation in Astronomy VI, ed. D.L. Crawford, 627, 733
- Tody, D. 1993, ADASS II, A.S.P. Conference Ser., Vol 52, eds. R.J. Hanisch, R.J.V. Brissenden, & J. Barnes, 173 p

Valdes, F., & Tody, G. 1998, Proceedings of SPIE Vol. 3355

Valdes, F. 1998, ADASS VII, ASP Conf. Series 145, ed. R. Albrect

Wolfe, A. M., Turnshek, D. A., Lanzetta, K. M., & Oke, J. B. 1992, ApJ 385, 151

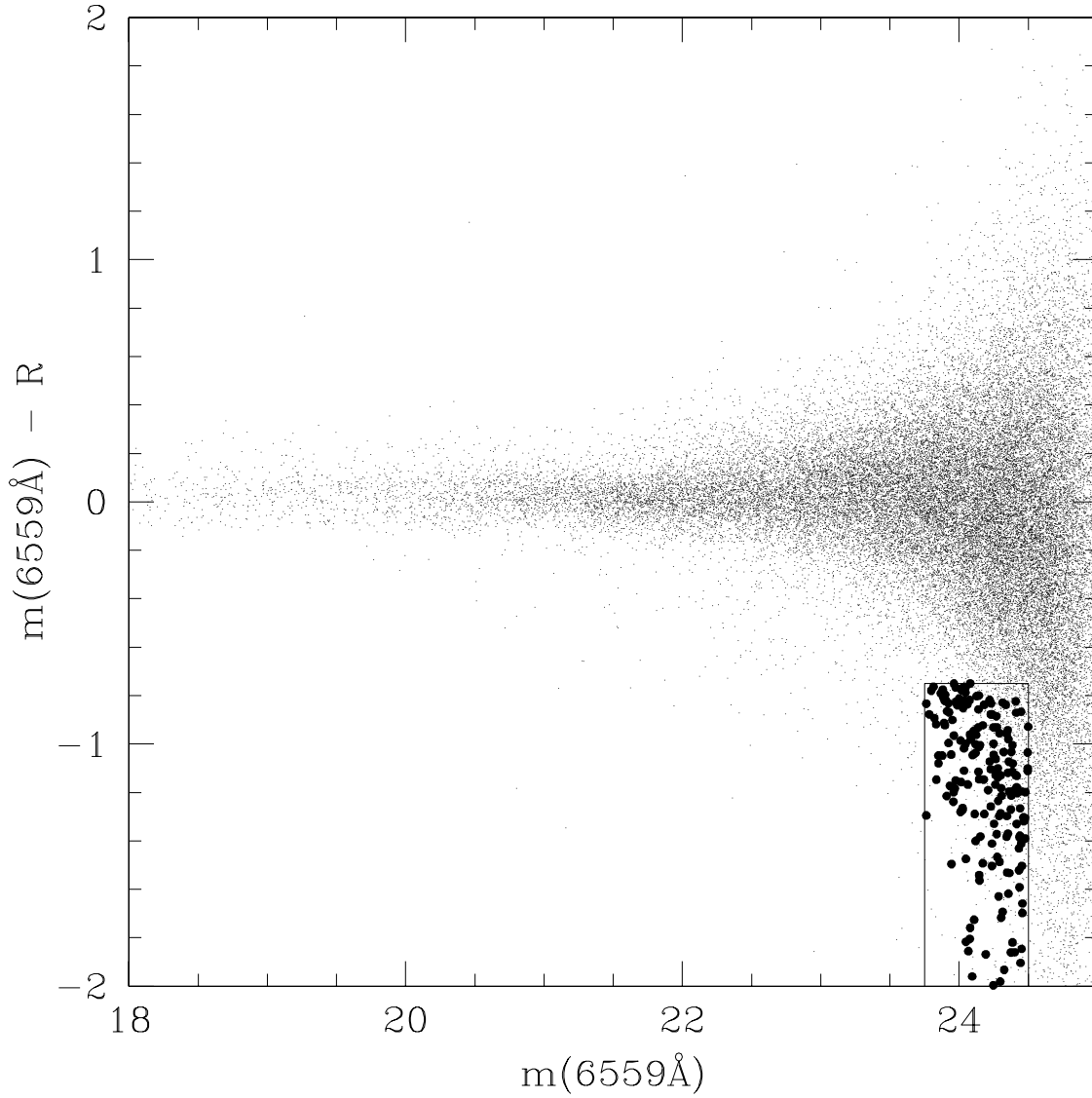


Fig. 1.— A sample LALA survey color-magnitude diagram, for narrowband 6559\AA magnitude (80\AA bandpass) and $6559\text{\AA} - R$ color. The zero point of the narrowband filter is calibrated using R band standard star fluxes (Landolt 1992), so that $m(6559\text{\AA}) = R$ for a pure continuum source of average spectral slope. The box in the lower right hand corner shows the color and magnitude constraints for good Lyman- α candidates, as described in the text. Additional constraints on the color error eliminate some objects meeting the color-magnitude cut; the final sample of good candidates for this filter is marked by the heavy points.

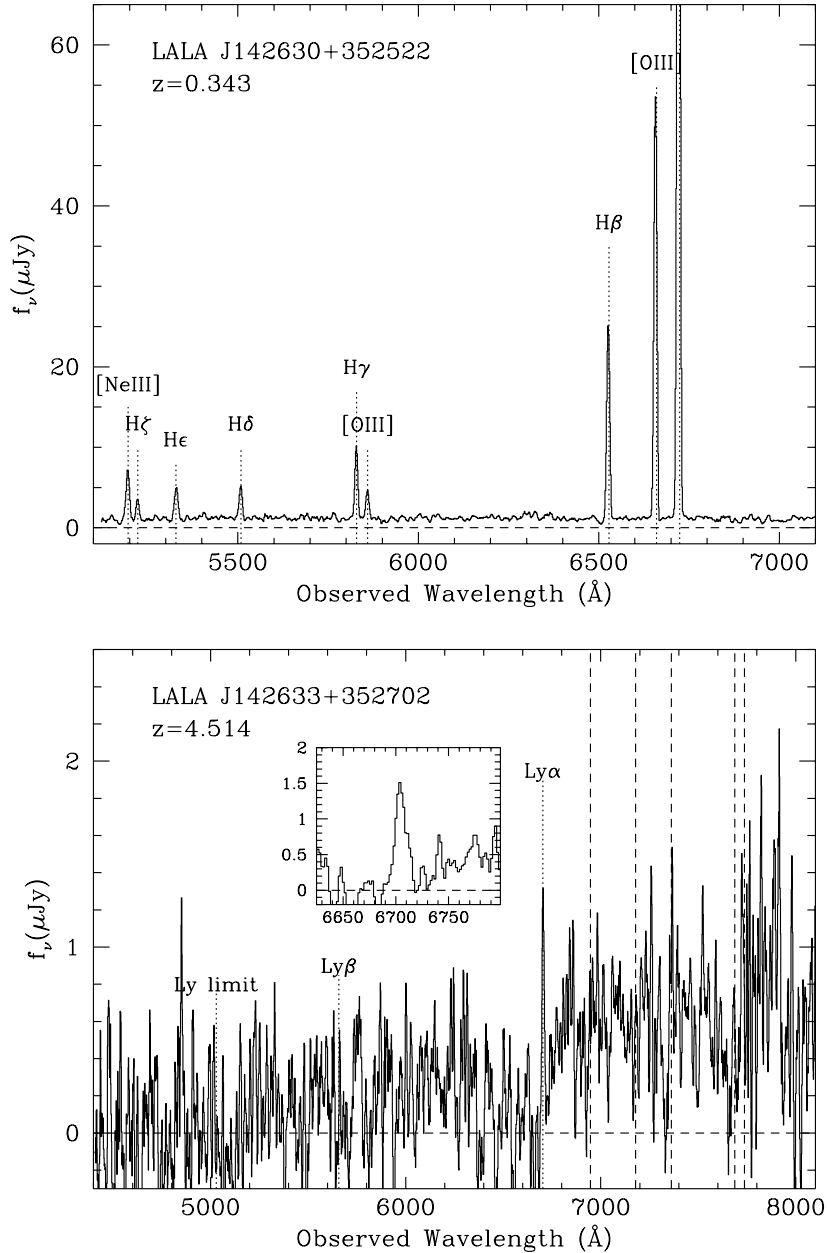


Fig. 2.— Keck spectra of two LALA emission line candidates. Top: The largest equivalent width source in the spectroscopic sample, a $z = 0.34$ OIII emitter with observed $\text{EW} \approx 1400\text{\AA}$. This source has eleven detected emission lines, and an [O III] $\lambda 5007\text{\AA}$ line luminosity of $2.5 \times 10^{41} \text{ergs}^{-1}$. It demonstrates our ability to find unusual objects through our large volume coverage. Bottom: A confirmed $z = 4.516$ Lyman- α source. This object has a line flux of $1.7 \times 10^{-17} \text{erg cm}^{-2} \text{s}^{-1}$ and an equivalent width of 84\AA . The line is asymmetric and has a strong continuum decrement from the red to the blue side, both of which are expected for high-redshift Lyman- α emitters (Stern & Spinrad 1999). It demonstrates our ability to find the faint Lyman- α emitter population.